

RESEARCH ARTICLE

Catalytic inhibition of KDM1A in Ewing sarcoma is insufficient as a therapeutic strategy

Antonio Romo-Morales¹  | Ewa Aladowicz¹ | Julian Blagg² | Susanne A. Gatz^{1,3} | Janet M. Shipley¹

¹Sarcoma Molecular Pathology Team, Divisions of Molecular Pathology and Cancer Therapeutics, The Institute of Cancer Research, London, UK

²Cancer Research UK Cancer Therapeutics Unit, Division of Cancer Therapeutics, The Institute of Cancer Research, London, UK

³Cancer Research UK Clinical Trials Unit, Institute of Cancer and Genomic Sciences, University of Birmingham, Edgbaston, Birmingham, UK

Correspondence

Janet Shipley, Sarcoma Molecular Pathology Team, Divisions of Molecular Pathology and Cancer Therapeutics, 15 Cotswold Road, Sutton, Surrey SM2 5NG, UK.
Email: janet.shipley@icr.ac.uk

Funding information

This work was supported by a studentship for AR from The Institute of Cancer Research, London and the Elin Rose Appeal. EA had support from the Tom Bowdidge Foundation and SAG had support from the Hopkins family.

SAG and JMS share senior authorship and contributed equally to this work.

Abstract

Background: Ewing sarcoma and desmoplastic small round cell tumors (DSRCT) are rare and clinically aggressive sarcomas usually characterized by oncogenic fusion proteins involving EWS. Emerging studies of Ewing sarcoma have demonstrated EWS-FLI1-driven chromatin remodeling as a key aspect of tumorigenicity. In particular, the lysine-specific demethylase KDM1A/LSD1 is linked to transcriptional regulation of target genes orchestrated by the EWS portion of the fusion protein interacting with repressive chromatin-remodeling complexes. Consistent with this model, depletion of KDM1A supports it is a molecular therapeutic target in Ewing sarcoma cells, but effective drugs need to be identified.

Procedure: A comprehensive phenotypic analysis of the effects of catalytic KDM1A inhibitors ORY-1001 and GSK2879552, including clinically relevant doses, was carried out in 2D and 3D spheroid models of Ewing sarcoma and DSRCT.

Results: Catalytic inhibition of KDM1A did not affect cell viability in 2D and 3D assays and had no impact on invasion in a 3D assay.

Conclusions: Overall, evidence presented here does not support inhibition of KDM1A catalytic demethylase activity as an effective therapeutic strategy for Ewing sarcoma or DSRCT. However, roles of KDM1A beyond its demethylase activity should be considered for these sarcomas.

KEYWORDS

3D models, Ewing sarcoma, GSK2879552, histone demethylase, KDM1A/LSD1, ORY-1001

1 | INTRODUCTION

Ewing sarcoma is a rare and highly aggressive sarcoma affecting children and young adults. Recent developments in our understanding of the molecular mechanisms underlying this disease have not yet translated into significant improvements in patients' outcomes, and treatment has remained unchanged.¹

Ewing sarcoma is characterized by chromosomal rearrangements between the gene *EWSR1* and gene members of the ETS-domain family

of transcription factors; approximately 85% to 90% of Ewing sarcoma tumors exhibit *FLI1* as the *EWSR1* fusion partner.² Additional *EWSR1* chromosomal translocations exist, such as fusion with *WT1*, found in 95% of cases of desmoplastic small round cell tumor (DSRCT).^{3,4}

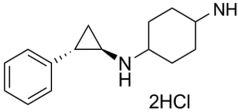
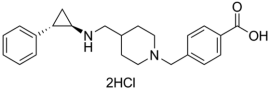
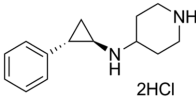
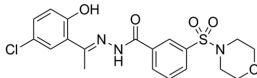
EWS-FLI1 has been identified as the main driver of Ewing sarcoma tumorigenicity through unique pioneer properties that increase genome-wide chromatin accessibility at GGAA microsatellite repeats.⁵⁻⁷ This is achieved through histone-modifying enzymes and chromatin-remodeling complexes changing the epigenetic status

Abbreviations: 3D, three-dimensional; AML, acute myeloid leukemia; ANOVA, analysis of variance; CHD, chromodomain; DSRCT, desmoplastic small round cell tumor; EWSR1, EWS RNA binding protein 1; EZH2, enhancer of zeste homolog 2; FLI1, friend leukemia integration 1; H3K4, histone 3 lysine 4; HDAC, histone deacetylase; KDM1A (LSD1), lysine-specific demethylase; MTA1, metastasis-associated protein; MTS, 3-(4,5-dimethyl-2-yl)-5-(3-carboxymethoxyphenyl)-2-(4-sulfophenyl)-2H-tetrazolium, inner salt; NuRD, nucleosome remodeling deacetylase complex; PVDF, polyvinylidene fluoride; SCLC, small cell lung cancer; SDS, sodium dodecyl sulfate; ULA, ultra-low attachment; WT1, Wilms tumor.

This is an open access article under the terms of the Creative Commons Attribution License, which permits use, distribution and reproduction in any medium, provided the original work is properly cited.

© 2019 The Authors. *Pediatric Blood & Cancer* Published by Wiley Periodicals, Inc.

TABLE 1 KDM1A inhibitors

Compound	ORY-1001	GSK2879552	GSK-LSD1	SP2509
Structure				
IC ₅₀ : 18 nM		K _{iapp} of 1.7 μM	IC ₅₀ : 16 nM	IC ₅₀ : 13 nM
Mechanism of action	Irreversible inhibitor covalently modifying the FAD cofactor (22)	Irreversible inhibitor covalently modifying the FAD cofactor (23)	Irreversible inhibitor covalently modifying the FAD cofactor (23)	Reversible noncompetitive inhibitor (43)
Clinical status	Phase I/IIa study in AML (EudraCT Number: 2013-002447-29) and SCLC (NCT02913443)	Phase I studies in SCLC (NCT02034123) and AML (NCT02177812) have been terminated because the risk benefit does not favor continuation. Phase I/II study in MDS (NCT02929498)	NA	NA

of genomic regions and creating de novo enhancer elements that establish the Ewing sarcoma transcriptional signature.^{8–10} In particular, the nucleosome remodeling deacetylase complex (NuRD; also known as Mi-2), a multi-subunit chromatin-remodeling complex commonly associated with repression of transcriptional activity, was identified to be relevant in the silencing of EWS-FLI1 target genes.^{10,11} Essentially, the catalytic activity in the NuRD complex involves deacetylation by histone deacetylase 2 (HDAC2) and 3 (HDAC3), coupled with demethylation by lysine-specific demethylase 1 (KDM1A; also referred to as LSD1, AOF2, and BHC110).^{9,10}

The working model proposed by Sankar et al consists of EWS-FLI1 binding to promoters of repressed target genes, followed by the recruitment of the NuRD complex through interaction between its subunits chromodomain 4 (CHD4) and metastasis-associated protein 1 (MTA1) and the EWS portion of the fusion protein. Following treatment with SP2509, a tool compound targeting KDM1A, the EWS-FLI1-driven transcriptional signature of both upregulated and downregulated genes was reversed.¹⁰ Inhibition of KDM1A with SP2509 also resulted in apoptosis and disruption of the oncogenic phenotype.¹⁰

KDM1A is a well-characterized histone lysine demethylase belonging to the family of flavin-dependent amine oxidases that has an important role in stem cell maintenance through transcriptional repression.^{12–14} This demethylase is also overexpressed in Ewing sarcoma and other sarcomas including DSRCT and rhabdomyosarcoma.^{15–17} Moreover, the key role of the EWS portion of the fusion protein in the interaction with repressive chromatin-remodeling complexes makes inclusion of DSRCT, possessing the EWS-WT1 fusion, relevant to study alongside EWS-FLI1 in Ewing sarcoma.^{8,9}

Currently, the KDM1A inhibitor ORY-1001 is being investigated in the clinic in adult patients with acute myeloid leukemia (AML) and small cell lung cancer (SCLC). In addition, a trial with GSK2879552 has recently been stopped citing that the benefits do not outweigh the risk in relapsed refractory SCLC^{18–21} (Table 1). These compounds are potent irreversible inhibitors of KDM1A, which covalently modify the FAD cofactor of this demethylase to inhibit catalytic activity.^{22,23}

However, their use as a therapeutic strategy for Ewing sarcoma has not been comprehensively assessed. Given the rationale for targeting KDM1A in Ewing sarcoma, in this work, we sought to test the potential for repurposing these clinical candidates against KDM1A as a novel treatment for these sarcomas.

The current report investigates the effect of catalytic inhibitors of KDM1A on cell viability in 2D and 3D models, and invasion using a 3D spheroid assay. Importantly, we show that clinically available inhibitors of KDM1A catalytic demethylase activity, despite having an effect on viability at a low nanomolar range against leukemia cell lines, do not have an effect in preclinical models of Ewing sarcoma and DSRCT. Therefore, catalytic inhibition of KDM1A should not be considered as a therapeutic strategy for Ewing sarcoma.

2 | METHODS

2.1 | Cell lines

Ewing sarcoma cell lines A673 and TC71 were kindly provided by Dr. Enrique de Álava (IBiS, Spain). The desmoplastic small round cell tumor cell line JN-DSRCT-1²⁴ was obtained from Sean B. Lee, and leukemia cell lines MV(4;11) and MOLT-4 were obtained from DSMZ, Germany. Cell lines used were cultured in the appropriate media supplemented with 10% fetal bovine serum (Gibco, Thermo Fisher Scientific, UK), 1% penicillin–streptomycin (Gibco), and 1% GlutaMAX (Gibco) in a humidified incubator at 37°C and 5% CO₂. Standard procedures were utilized for maintenance, freezing, and thawing. Cells were *Mycoplasma*-free tested with the Plasmotest Mycoplasma Detection Kit (InvivoGen, UK) according to instructions. Cell lines were authenticated with short tandem repeat testing using the GenePrint 10 system (Promega, UK).

2.2 | Reagents and drug treatments

The following KDM1A inhibitors were used: ORY-1001, GSK2879552, GSK-LSD1, and SP2509 (Table 1; SelleckChem, UK). Stocks (10 mM)

were prepared in H₂O for ORY-1001 and GSK2879552, and in DMSO for GSK-LSD1 and SP2509 and stored at –80°C.

2.3 | Cell viability assays

A673 cells were seeded at 2000 cells/well, TC71 cells at 4000 cells/well, and JN-DSRCT-1 at 4000 cells/well in 96-well plates for viability assays (six replicates for each condition). Viability was assessed by an MTS (3-(4,5-dimethyl-2-yl)-5-(3-carboxymethoxyphenyl)-2-(4-sulfophenyl)-2H-tetrazolium, inner salt) assay using the CellTiter 96 Aqueous One Solution Cell Proliferation Assay (Promega). Media were replaced with 100 μ L of Opti-MEM and 20 μ L of CellTiter 96 Aqueous One Solution Cell Proliferation Assay. Plates were incubated for two hours in normal culturing conditions prior to measuring the absorbance of each well at 492 nm.

For MV(4;11) and MOLT-4 viability assays, cells were seeded at 100 000/well (6-well plate) and cultured for the indicated time. Viable cell counts were determined by Trypan blue assay (Sigma-Aldrich, UK).

2.4 | 3D spheroid culture

Three-dimensional spheroids were generated and cultured using the GravityTRAP ULA Plate 96-well (PerkinElmer, UK) unless otherwise indicated. Prior to seeding, wells were pre-wet with 40 μ L of medium. One thousand cells in 70 μ L were seeded into each well. Plates were spun for two minutes at 250 RCF to remove trapped air bubbles. Routine medium changes were performed every 48 hours by carefully aspirating the medium from the ledge at the inside wall of the well and replenishing it with fresh medium.

2.5 | Image analysis of 3D spheroids

Digital images of spheroids were captured throughout the duration of the experiments using an IN Cell Analyzer 2200 imaging system (GE Healthcare Life Sciences, UK), and the surface area was assessed at the focal plane with maximum diameter with IN Cell Investigator IN Developer Toolbox (GE Healthcare Life Sciences).

2.6 | Western blot analysis

2.6.1 | H3K4me2 immunoblot

Following treatment, 2.5×10^5 cells were lysed with 50 μ L of 3 \times Laemmli buffer made up with 2 mL of 1 M Tris Base pH 6.8, 3 mL of 100% Glycerol, 8 mL of 10% SDS, 300 μ L of 1% bromophenol blue, and 400 μ L of β -mercaptoethanol (freshly added at the time of whole-cell lysate preparation).

Standard protein extraction with cell lysis buffer (Cell Signaling Technology, UK) and Western blot analysis techniques were used for remaining Western blots. Five to 30 micrograms of protein extract or 5 μ L of whole-cell lysate in 3X Laemmli buffer was loaded into wells of a NuPAGE 4% to 12% Bis-Tris protein gels (Invitrogen, Thermo Fisher Scientific, UK). Protein gels were transferred onto PVDF membranes with iBlot2 transfer stacks on the iBlot2 transfer system (Invitrogen)

following the manufacturer's instructions. The iBlot2 transfer system was run at 20 V for seven minutes.

Densitometry values for each band were normalized to total protein or housekeeping control of the control sample band and relative to the indicated control. Western blots are representative of at least two independent repeats.

2.7 | 3D invasion assay

A673 and TC71 cells were seeded at a density of 500 cells per well in ultra-low attachment (ULA) round-bottom 96-well plates (Corning, UK). After three days of culturing, spheroids were treated with KDM1A inhibitors at the indicated concentration for 10 days. Fifty microliters of medium was removed from each well and replaced with 50 μ L of fresh medium with drug every 48 hours. Following treatment, 50 μ L of medium was removed and carefully replaced with 50 μ L of Matrigel (Corning) containing drug, achieving a final concentration of Matrigel of 4.5 mg/mL. Plates were then incubated at 37°C and 5% CO₂ in an IncuCyte Zoom (Sartorius, UK) for 48 hours where images were taken every hour to monitor invasion.

2.8 | qRT-PCR

RNA was extracted with TRIzol according to the manufacturer's protocol.²⁵ A673 cell line cDNA was synthesized using the High Capacity cDNA Reverse Transcriptase kit (Applied Biosystems, CA, USA) following the manufacturer's instructions. Multiplex PCR reactions were set up in triplicate in 384-well optical-reaction PRC plates (Applied Biosystems) and run on a ViiA 7 Real-Time PCR System (Applied Biosystems, CA, USA). The following TaqMan probes were used: LOX Hs00942480_m1, TGFBR2 Hs00234253_m1, HMOX1 Hs01110250_m1, E2F1 Hs00153451_m1, and CAV1 Hs00971716_m1. Human RPLPO endogenous control (Applied Biosystems, CA, USA) was used to normalize gene expression.

2.9 | Statistical analysis

GraphPad PRISM 7 and R studio 3.3.2 were used to carry out the statistical analyses. Error bars represent means \pm standard deviation from various independent experiments as indicated in figure legends. Statistical significance was measured by one-way ANOVA with post hoc Sidak test for multiple comparisons and two-way ANOVA with post hoc Dunnett test and Sidak test where applicable. $P < 0.05$ was considered significant and indicated by *, $P < 0.01$ is indicated by **, $P < 0.001$ is indicated by ***, and $P < 0.0001$ is indicated by ****.

3 | RESULTS

Presently, there is no evidence demonstrating whether the clinical drug candidates for KDM1A have activity in preclinical models of Ewing sarcoma. To begin to address this question, Ewing sarcoma cell lines A673 and TC71 were treated with compounds for 96 hours to investigate the effect of KDM1A inhibition on cell viability. The cell lines tested

showed no sensitivity to treatment with the irreversible inhibitors of KDM1A demethylase function: ORY-1001 and GSK2879552 (Figure 1). Conversely, treatment with tool compound SP2509 revealed a rapid decrease in viability with GI50s in the submicromolar range (A673: 123 nM and TC71: 355 nM). Morphological assessment of cells following treatment with clinical drug candidates showed no differences between treated and untreated. Cell morphology in the SP2509-treated cells was consistent with apoptosis (Figure S1A).^{9,10} These effects were replicated in the DSRCT cell line, only showing sensitivity to SP2509 and not to the clinical drug candidates (Figure S1B). To address the discrepancy between the KDM1A inhibitors, a chemical probe validated as a potent and selective inhibitor of KDM1A catalytic demethylase activity (GSK-LSD1) was also tested in these sarcoma cell lines (<http://www.thesgc.org/chemical-probes/LSD1>).^{23,26} Again, treatment had no meaningful effect on cell viability, with only a 50% reduction at 10 μ M in one cell line (TC71; Figure 1; Supporting Information Figure S1C). KDM1A protein levels were unaffected following treatment with clinical drug candidates ORY-1001 and GSK2879552 after 48, 72, 96, and 168 hours (Supporting Information Figure S1D–S1E).

Importantly, consistent with their *in vitro* inhibition of KDM1A demethylase activity, all four compounds were able to modulate KDM1A-mediated demethylation of the H3K4 methyl mark, a well-characterized KDM1A substrate.¹⁵ Following 72 hours of treatment with 2 μ M for all drugs, including the tool compound GSK-LSD1, there was an increase in the global levels of H3K4me2 in both Ewing sarcoma cell lines (Figure 1 and 1D). Furthermore, to investigate the impact on EWS-FLI1-driven transcription, we selected downstream target genes of the fusion protein and assessed by qRT-PCR following treatment with ORY-1001 and GSK2879552. Extended exposure of up to two weeks (336 hours) was conducted to ensure prolonged catalytic inhibition. We did not observe a biologically relevant change in expression of five target genes at a range of time points following treatment with ORY-1001 and GSK2879552 at 2 and 10 μ M, despite statistical significance (Figure 1F). As a positive control, treatment with tool compound SP2509 (250 nM) reversed expression of *LOX* and *HMOX1* in agreement with previous reports, but not *TGFBR2* or EWS-FLI1 activated genes *E2F1* and *CAV1* (Supporting Information Figure S1F–S1H),^{9,10} possibly due to the lower concentration used in our experiments.

To further demonstrate compound activity, we assessed the response of leukemia cells, previously shown to be sensitive to inhibition of KDM1A catalytic function by ORY-1001 in the nanomolar range.²² In agreement with published findings, the clinical candidate ORY-1001, as well as chemical probe GSK-LSD1, showed a reduction in cell viability upon treatment with compound at 10 nM concentrations in two leukemia cell lines (Supporting Information Figure S2A and S2B). The clinical candidate GSK2879552 also decreased cell viability at 2 μ M (Supporting Information Figure S2C).

To perform a more comprehensive evaluation of the effect of KDM1A inhibition, assessment of cell viability experiments was expanded to 3D models of Ewing sarcoma. Three-dimensional cell culture systems have become more prominent in preclinical studies due to

their ability to more closely represent tissue compartments and enable longer experimental time frames.²⁷ Tumor spheroids, for example, can recapitulate aspects of the tumor microenvironment that ultimately influence drug response.²⁸ A673 spheroid cultures were treated with ORY-1001 and SP2509 for 10 days with a dose range between 0.3 and 10 μ M (Figure 2 and 2B). Again, no effect on growth was observed with the irreversible inhibitor of KDM1A catalytic function ORY-1001, whereas SP2509 was active, albeit at higher concentrations compared with 2D cultures (Figure 2 and 2B). Drugs targeting epigenetic modifying enzymes often require prolonged inhibition for maximal drug potency and response to treatment.^{22,23,29} We therefore additionally treated spheroids for up to 21 days with a maximum concentration of 100 μ M of both clinical candidates (ORY-1001 and GSK2879552). Both clinical candidates had no effect upon spheroid growth (Figure 2 and 2E), even in the extended assay.

Finally, KDM1A has been reported to have a role in migration and invasion.³⁰ To complete the phenotypic assessment of KDM1A inhibition, we evaluated if Ewing sarcoma cells showed a change in their invasive phenotype upon inhibition of KDM1A catalytic demethylase activity. A673 and TC71 spheroids were pretreated for 10 days with the KDM1A inhibitors, and subsequently cultured in a Matrigel matrix, in which invasion was monitored for a further 48 hours. A comparison of the total spheroid area indicated that KDM1A inhibition had no impact on the invaded area (Figure 3 and 3B; Supporting Information Figure S3). Consistent with our previous results, the measured spheroid area was not affected in the 10-day pretreatment with either 2 μ M or 10 μ M concentrations of compound (Figure 3; Supporting Information Figure S3). Again, we included the chemical probe GSK-LSD1 in the assay; it also had no effect on invasion (Figure 3 and 3B; Supporting Information Figure S3).

4 | DISCUSSION

The Ewing sarcoma gene-expression profile heavily relies on EWS-FLI1 coordinating vast epigenetic rewiring through the recruitment and activity of chromatin-remodeling complexes.^{7,8,31} In this context, KDM1A, an active subunit of the NuRD complex, has been reported to have an important role in repressing and activating target genes of the fusion protein EWS-FLI1.^{9,10} The functional role of KDM1A in Ewing sarcoma oncogenesis, alongside high expression in this and other sarcomas such as DSRCT, has made it a promising therapeutic target.^{32,33} In light of this, our aim was to assess the therapeutic potential of KDM1A inhibitors (ORY-1001 and GSK2879552) in Ewing sarcoma models.

Global or promoter-specific accumulation of methylation of H3K4 is not always seen following KDM1A inhibition regardless of decreased KDM1A activity.^{23,34} However, in our findings, the global change in H3K4me2 upon treatment with all KDM1A inhibitors demonstrated capacity to effectively inhibit KDM1A catalytic activity. Importantly, this did not translate into reversal of expression of EWS-FLI1 downstream target genes by ORY-1001 and GSK2879552 analyzed by qRT-PCR.

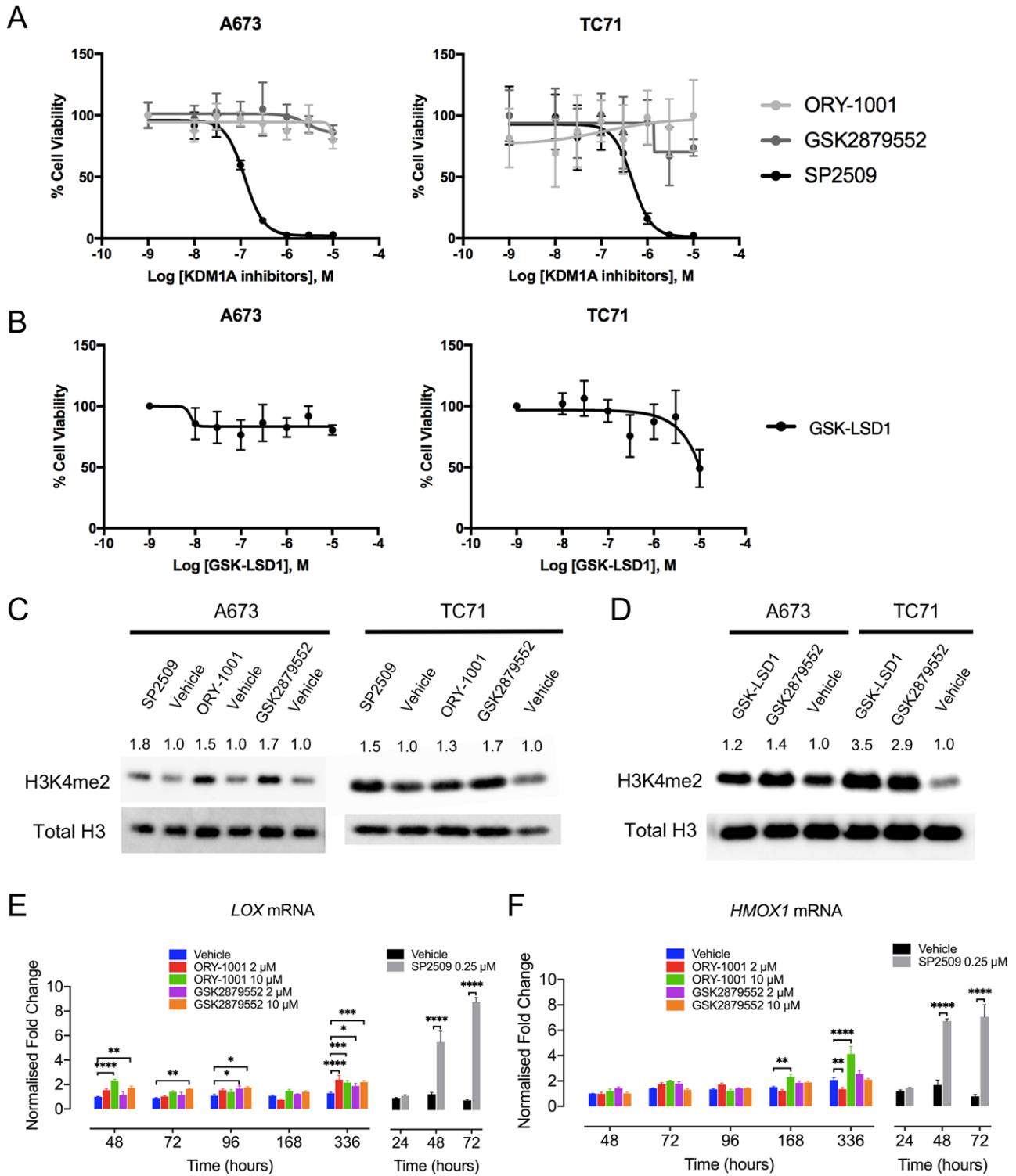


FIGURE 1 Effects of KDM1A inhibition on Ewing sarcoma cell lines. (A–B) Ewing sarcoma cell lines A673 and TC71 were exposed to a range of concentrations of KDM1A inhibitors for 96 hours. Cell viability was assessed by MTS assay. Means \pm SD of 6 replicates; graphs are representative of three independent repeats. (C–D) Western blot of H3K4me2 of A673 and TC71 cell lines treated with KDM1A inhibitors (SP2509, ORY-1001, GSK2879552, and GSK-LSD1) (2 μ M) and their respective vehicle controls. Densitometry values shown above each blot were normalized to total H3 and relative to each vehicle control. Western blots are representative of at least two independent repeats. (E–F) Effect of KDM1A inhibitors on EWS-FLI1 target genes expression. qRT-PCR analysis of *LOX* and *HMOX1* in A673 cells treated with vehicle or KDM1A inhibitors ORY-1001 (2 μ M, 10 μ M), GSK2879552 (2 μ M, 10 μ M), and SP2509 (250 nM). Normalized fold change was adjusted to human *RPLPO* endogenous control. Means \pm SD of three replicates. Data are representative of two independent repeats. Statistical analysis: two-way ANOVA with Dunnett and Sidak multiple comparisons test, not significant comparisons are not shown; * $P < 0.05$; ** $P < 0.01$; *** $P < 0.001$; **** $P < 0.0001$

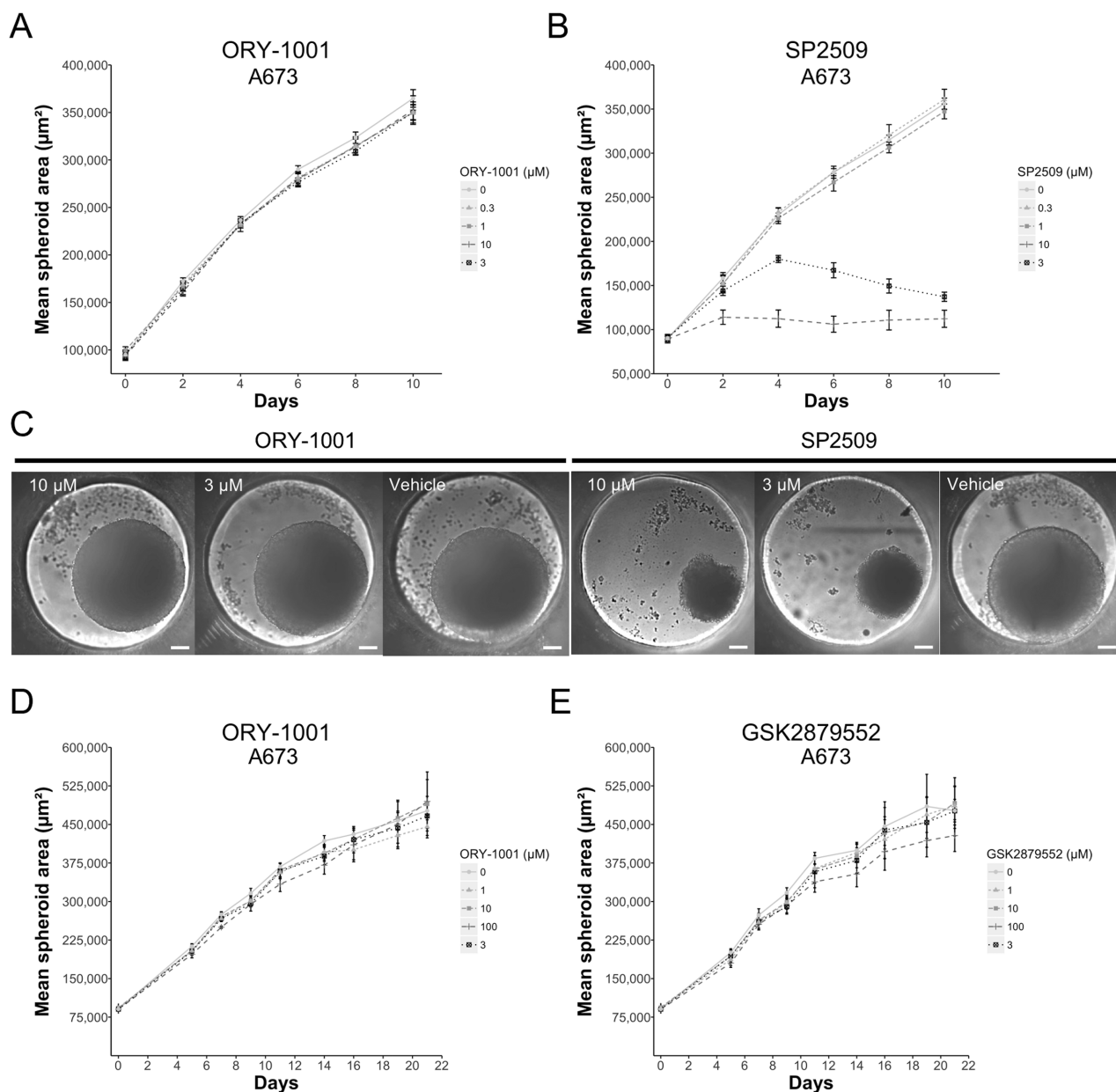


FIGURE 2 Effect of KDM1A inhibitors on the cell proliferation of Ewing sarcoma spheroids. Growth curve of A673 spheroids treated with a range of concentrations of KDM1A inhibitors ORY-1001 (A) and SP2509 (B) for 10 days. (C) Wells containing representative spheroids at day 10 of treatment with ORY-1001 and SP2509 at 10 μ M, 3 μ M, and vehicle, respectively. Scale bars: 100 μ m. Long-term treatment of A673 spheroids with clinical candidates ORY-1001 (D) and GSK2879552 (E) for 21 days. Maximum area at greater width of a sphere was measured in images taken over the different time courses. Means \pm SD of 6–10 replicates

Catalytic inhibition of KDM1A with the clinical drug candidates ORY-1001 and GSK2879552 reproduced the reported decrease in cell viability in leukemia cell lines.²² On the other hand, repurposing of these clinical compounds for Ewing sarcoma did not exhibit anticancer activity in 2D and 3D viability assays even at concentrations up to 100 μ M. A validated potent and selective chemical probe for inhibition of KDM1A catalytic function (<http://www.thesgc.org/chemical-probes/LSD1>),^{23,26} which shares the same chemical scaffold with the clinical candidate compounds and has the same mechanism of action through irreversible covalent modification of the FAD cofactor, also had no effect on the cell viability of Ewing sarcoma cells in 2D

and 3D. Prolonged inhibition, as a means to achieve maximal efficacy, as in reports with inhibitors of Enhancer of Zeste Homolog 2 (EZH2) in lymphoma, did not alter the response to these inhibitors of KDM1A catalytic function.^{22,23,29}

KDM1A's reported role in modulating self-renewal and differentiation in embryonic stem cells also encompasses regulation of migration during normal mammalian development.^{14,35} Importantly, in solid tumors, high levels of KDM1A have been associated with metastasis, and inhibition of this demethylase has been shown to attenuate migration and invasion in breast cancer cell lines.³⁰ Metastasis is a key problem in Ewing sarcoma with patients with disseminated

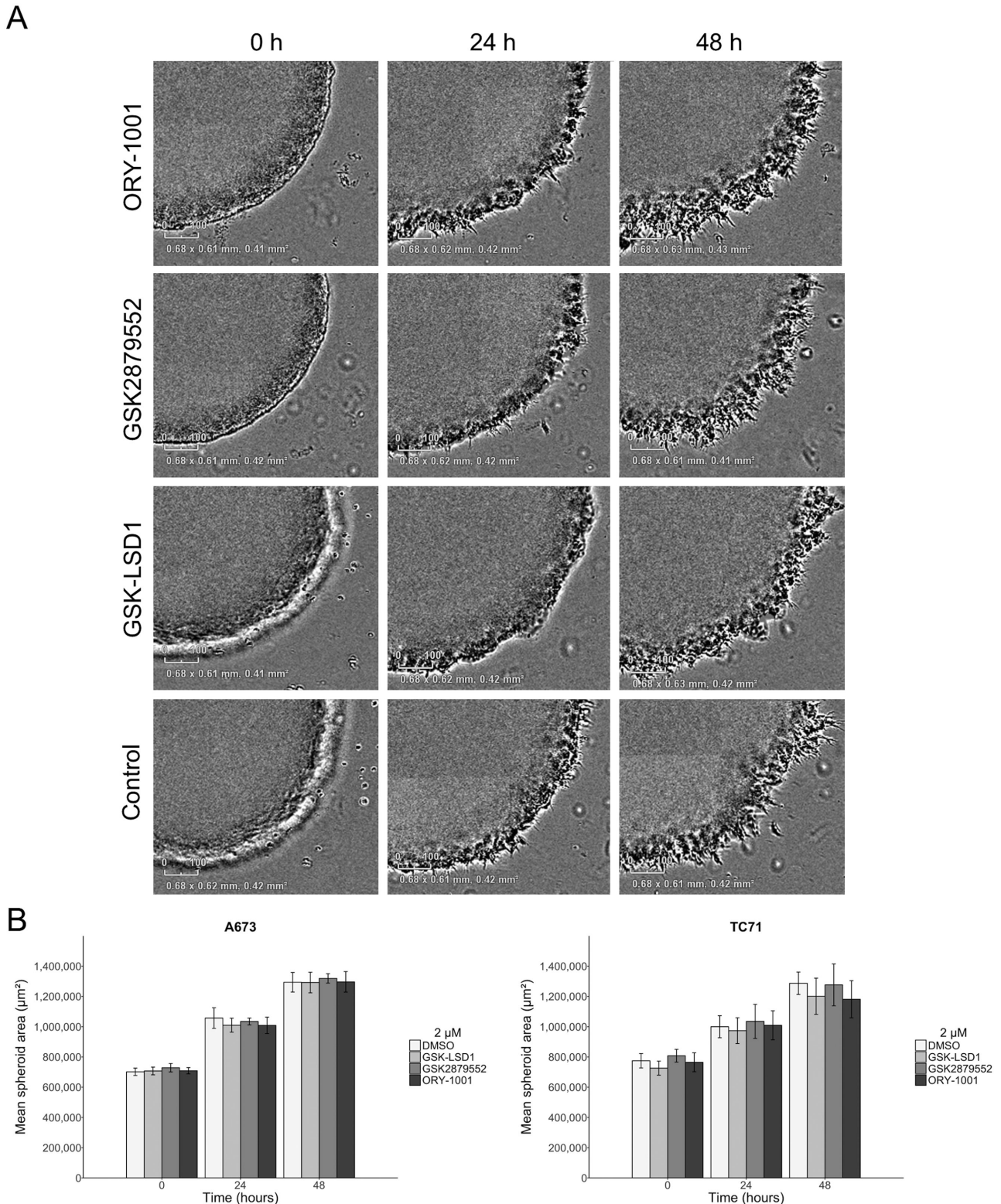


FIGURE 3 Effects of KDM1A inhibitors on the invasion of Ewing sarcoma spheroids. (A) Three-dimensional spheroid invasion assay with Ewing sarcoma cell lines A673 spheroids pretreated with KDM1A clinical drug candidates: ORY-1001 and GSK2879552 and tool compound GSK-LSD1 for 10 days (2 μ M). (B) A673 and TC71 total spheroid area measured with IncuCyte ZOOM software for 48 hours (10-day pretreatment with 2 μ M). Means \pm SD of 3–5 replicates; graphs are representative of two independent repeats. Statistical analysis: two-way ANOVA and Dunnett multiple comparison test, $P < 0.05$ between drugs tested within the same time point

disease showing dismal survival below 30%.³⁶ Therefore, investigating invasion as part of the phenotypic assessment of KDM1A inhibition was highly relevant. However, in our 3D invasion assay, KDM1A inhibition did not alter the invasive phenotype, and it particularly failed to suppress invasion in Ewing sarcoma spheroids.

The disease context and the nature of the role that KDM1A plays in various malignancies are key determinants of KDM1A inhibition as a therapeutic strategy. In leukemia, KDM1A demethylase activity acts as a key silencer of regulators of hematopoiesis, essential in maintaining leukemia stem cells.³⁷ This transcriptional repression and differentiation arrest can be relieved through inhibition of KDM1A catalytic function or protein knockdown.^{22,37} However, in the context of Ewing sarcoma, despite the observed change in the methylation levels of H3K4, inhibition of KDM1A catalytic function was insufficient to modulate a selection of known target genes of EWS-FLI and impair Ewing sarcoma cells survival. This suggests catalytic activity of KDM1A may not contribute to establishing EWS-FLI1's transcriptional program. Recent findings showed that shRNA-mediated depletion of KDM1A in Ewing sarcoma cells resulted in severe growth impairment and cell death, confirming their dependency on this demethylase.³⁸ The discrepancy between our results through inhibition of KDM1A catalytic function and knockdown of the multidomain protein strongly suggests a non-canonical role for KDM1A, independent from its demethylase function. These characteristics coincide with other epigenetic regulators such as EZH2. Its emerging methyltransferase- and polycomb-independent roles provide novel therapeutic potential for inhibitors disrupting its docking capacity.³⁹

In line with this model, recent reports in prostate cancer cell lines described a scaffolding role for KDM1A, whereby catalytically inactive KDM1A was still able to establish the prostate cancer gene network and ensure survival of castration-resistant prostate cancer cell lines.⁴⁰ This was further confirmed with the tool compound SP2509, proposed as an allosteric inhibitor binding to the H3 pocket region of KDM1A, capable of inducing cell death in prostate cancer cell lines. Similarly, this could also explain the previously observed reversal of the EWS-FLI1 signature effects with SP2509 in Ewing sarcoma cells.¹⁰ However, it is noteworthy that SP2509 has been shown to effectively cause cell death regardless of KDM1A expression in a leukemia KDM1A knockout cell line and its isogenic control.⁴¹ In addition to disrupting KDM1A's complex formation capabilities, SP2509 may have additional cytotoxic effects independent from KDM1A binding. Consistent with this, 2-hydroxyphenyl-hydrazone structural motif within SP2509 has previously been identified as a pan-assay interference flag and has the potential to elicit promiscuous biological activity.⁴²⁻⁴⁴ KDM1A's role as a docking element for additional proteins may play a more prominent part in Ewing sarcoma cells survival than previously considered.¹⁵

Our work is particularly timely and pertinent as a drug of the same mechanistic class of KDM1A inhibitors as the irreversible KDM1A demethylase inhibitors tested here has entered phase I trials in Ewing sarcoma patients (NCT03514407). In summary, we demonstrate that the clinical candidates ORY-1001 and GSK2879552, which act predominantly as inhibitors of KDM1A catalytic function, are not effective against *in vitro* models of Ewing sarcoma. The data presented here do

not support clinical trials exploring inhibition of KDM1A demethylase function as a therapeutic strategy for the treatment of Ewing sarcoma and DSRCT.

ACKNOWLEDGMENTS

We are grateful to our funders whose support made this work possible: the Elin Rose Appeal (AR), the Tom Bowdidge Foundation (EA), and the Hopkins family (SAG).

CONFLICTS OF INTEREST

The authors declare no conflicts of interest.

AUTHORS' CONTRIBUTIONS

AR conducted the experiments and analyzed data. AR, EA, SAG, JS designed the project. SAG and JS supervised the project. AR drafted the manuscript and all authors participated in writing the manuscript and approved the final version.

DATA AVAILABILITY STATEMENT

The data that support the findings of this study are available from the corresponding author upon reasonable request.

ORCID

Antonio Romo-Morales  <https://orcid.org/0000-0003-1779-7178>

REFERENCES

1. Grunewald TGP, Cidre-Aranaz F, Surdez D, et al. Ewing sarcoma. *Nat Rev Dis Primers*. 2018;4(1):5.
2. Delattre O, Zucman J, Plougastel B, et al. Gene fusion with an ETS DNA-binding domain caused by chromosome translocation in human tumours. *Nature*. 1992;359(6391):162-165.
3. Gerald WL, Haber DA. The EWS-WT1 gene fusion in desmoplastic small round cell tumor. *Semin Cancer Biol*. 2005;15(3):197-205.
4. Kovar H, Dr. Jekyll and Mr. Hyde: the two faces of the FUS/EWS/TAF15 protein family. *Sarcoma*. 2011;2011:837474.
5. Gangwal K, Close D, Enriquez CA, Hill CP, Lessnick SL. Emergent properties of EWS/FLI regulation via GGAA microsatellites in Ewing's sarcoma. *Genes Cancer*. 2010;1(2):177-187.
6. Gangwal K, Sankar S, Hollenhorst PC, et al. Microsatellites as EWS/FLI response elements in Ewing's sarcoma. *Proc Natl Acad Sci U S A*. 2008;105(29):10149-10154.
7. Riggi N, Knoechel B, Gillespie SM, et al. EWS-FLI1 utilizes divergent chromatin remodeling mechanisms to directly activate or repress enhancer elements in Ewing sarcoma. *Cancer Cell*. 2014;26(5):668-681.
8. Boulay G, Sandoval GJ, Riggi N, et al. Cancer-specific retargeting of BAF complexes by a prion-like domain. *Cell*. 2017;171(1):163-178.e19.
9. Sankar S, Bell R, Stephens B, et al. Mechanism and relevance of EWS/FLI-mediated transcriptional repression in Ewing sarcoma. *Oncogene*. 2013;32(42):5089-5100.
10. Sankar S, Theisen ER, Bearss J, et al. Reversible LSD1 inhibition interferes with global EWS/ETS transcriptional activity and impedes Ewing sarcoma tumor growth. *Clin Cancer Res*. 2014;20(17):4584-4597.

11. Lai AY, Wade PA. Cancer biology and NuRD: a multifaceted chromatin remodelling complex. *Nat Rev Cancer*. 2011;11(8):588-596.
12. Maiques-Diaz A, Somerville TC. LSD1: biologic roles and therapeutic targeting. *Epigenomics*. 2016;8(8):1103-1116.
13. Shi Y, Lan F, Matson C, et al. Histone demethylation mediated by the nuclear amine oxidase homolog LSD1. *Cell*. 2004;119(7):941-953.
14. Adamo A, Sese B, Boue S, et al. LSD1 regulates the balance between self-renewal and differentiation in human embryonic stem cells. *Nat Cell Biol*. 2011;13(6):652-659.
15. Forneris F, Binda C, Vanoni MA, Battaglioli E, Mattevi A. Human histone demethylase LSD1 reads the histone code. *J Biol Chem*. 2005;280(50):41360-41365.
16. Bennani-Baiti IM, Machado I, Llombart-Bosch A, Kovar H. Lysine-specific demethylase 1 (LSD1/KDM1A/AOF2/BHC110) is expressed and is an epigenetic drug target in chondrosarcoma, Ewing's sarcoma, osteosarcoma, and rhabdomyosarcoma. *Hum Pathol*. 2012;43(8):1300-1307.
17. Schildhaus HU, Riegel R, Hartmann W, et al. Lysine-specific demethylase 1 is highly expressed in solitary fibrous tumors, synovial sarcomas, rhabdomyosarcomas, desmoplastic small round cell tumors, and malignant peripheral nerve sheath tumors. *Hum Pathol*. 2011;42(11):1667-1675.
18. Safety, clinical activity, pharmacokinetics (PK) and pharmacodynamics study of GSK2879552, alone or with azacitidine, in subjects with high risk myelodysplastic syndromes (MDS). Available from: <https://clinicaltrials.gov/ct2/show/NCT02929498?term=GSK2879552&NLM=identifier:NCT02929498>.
19. Investigation of GSK2879552 in subjects with relapsed/refractory small cell lung carcinoma. Available from: <https://clinicaltrials.gov/ct2/show/NCT02034123?term=GSK2879552&rank=2>. NLM identifier: NCT02034123.
20. A phase I dose escalation study of GSK2879552 in subjects with acute myeloid leukemia (AML). Available from: <https://clinicaltrials.gov/ct2/show/NCT02177812?term=KDM1A+inhibitors>. NLM identifier: NCT02177812.
21. A dose finding and expansion study of RO7051790 administered orally in participants with relapsed, extensive-stage disease small cell lung cancer (ED SCLC). Available from: <https://clinicaltrials.gov/ct2/show/NCT02913443?term=RO7051790&rank=1>. NLM identifier: NCT02913443.
22. Maes T, Mascaro C, Tirapu I, et al. ORY-1001, a potent and selective covalent KDM1A inhibitor, for the treatment of acute leukemia. *Cancer Cell*. 2018;33(3):495-511. e412.
23. Mohammad HP, Smitheman KN, Kamat CD, et al. A DNA hypomethylation signature predicts antitumor activity of LSD1 inhibitors in SCLC. *Cancer Cell*. 2015;28(1):57-69.
24. Nishio J, Iwasaki H, Ishiguro M, et al. Establishment and characterization of a novel human desmoplastic small round cell tumor cell line, JN-DSRCT-1. *Lab Invest*. 2002;82(9):1175-1182.
25. Rio DC, Ares M, Hannon GJ, Nilsen TW. Purification of RNA using TRIzol (TRI reagent). *Cold Spring Harbor Protocols*. 2010;2010(6). pdb.prot5439.
26. The Structural Genomics Consortium. GSK-LSD1. A chemical probe for LSD1. *Chemical Probes* 2014; <https://www.thesgc.org/chemical-probes/GSK-LSD1>. Accessed 12 July, 2018.
27. Langhans SA. Three-dimensional in vitro cell culture models in drug discovery and drug repositioning. *Front Pharmacol*. 2018;9:6.
28. Riffle S, Pandey RN, Albert M, Hegde RS. Linking hypoxia, DNA damage and proliferation in multicellular tumor spheroids. *BMC Cancer*. 2017;17(1):338.
29. McCabe MT, Ott HM, Ganji G, et al. EZH2 inhibition as a therapeutic strategy for lymphoma with EZH2-activating mutations. *Nature*. 2012;492(7427):108-112.
30. Wang Y, Zhang H, Chen Y, et al. LSD1 is a subunit of the NuRD complex and targets the metastasis programs in breast cancer. *Cell*. 2009;138(4):660-672.
31. Riggi N, Suva ML, Suva D, et al. EWS-FLI-1 expression triggers a Ewing's sarcoma initiation program in primary human mesenchymal stem cells. *Cancer Res*. 2008;68(7):2176-2185.
32. Pishas KI, Lessnick SL. Recent advances in targeted therapy for Ewing sarcoma. *F1000Res*. 2016;5. pii: F1000 Faculty Rev-2077.
33. Theisen ER, Pishas KI, Saund RS, Lessnick SL. Therapeutic opportunities in Ewing sarcoma: EWS-FLI inhibition via LSD1 targeting. *Oncotarget*. 2016;7(14):17616-17630.
34. Maiques-Diaz A, Spencer GJ, Lynch JT, et al. Enhancer activation by pharmacologic displacement of LSD1 from GFI1 induces differentiation in acute myeloid leukemia. *Cell Rep*. 2018;22(13):3641-3659.
35. Zhu D, Holz S, Metzger E, et al. Lysine-specific demethylase 1 regulates differentiation onset and migration of trophoblast stem cells. *Nat Commun*. 2014;5:3174.
36. Kovar H, Alonso J, Aman P, et al. The first European interdisciplinary Ewing sarcoma research summit. *Front Oncol*. 2012; 2:54.
37. Harris WJ, Huang X, Lynch JT, et al. The histone demethylase KDM1A sustains the oncogenic potential of MLL-AF9 leukemia stem cells. *Cancer Cell*. 2012;21(4):473-487.
38. Pishas KI, Drenberg CD, Taslim C, et al. Therapeutic targeting of KDM1A/LSD1 in Ewing sarcoma with SP-2509 engages the endoplasmic reticulum stress response. *Mol Cancer Ther*. 2018.
39. Kim J, Lee Y, Lu X, et al. Polycomb- and methylation-independent roles of EZH2 as a transcription activator. *Cell Rep*. 2018;25(10):2808-2820. e2804.
40. Sehrawat A, Gao L, Wang Y, et al. LSD1 activates a lethal prostate cancer gene network independently of its demethylase function. *Proc Natl Acad Sci U S A*. 2018;115(18):E4179-E4188.
41. Sonnemann J, Zimmermann M, Marx C, et al. LSD1 (KDM1A)-independent effects of the LSD1 inhibitor SP2509 in cancer cells. *Br J Haematol*. 2018;183(3):494-497.
42. Baell JB, Holloway GA. New substructure filters for removal of pan assay interference compounds (PAINS) from screening libraries and for their exclusion in bioassays. *J Med Chem*. 2010;53(7):2719-2740.
43. Hitchin JR, Blagg J, Burke R, et al. Development and evaluation of selective, reversible LSD1 inhibitors derived from fragments. *Medchemcomm*. 2013;4(11):1513-1522.
44. Mould DP, McGonagle AE, Wiseman DH, Williams EL, Jordan AM. Reversible inhibitors of LSD1 as therapeutic agents in acute myeloid leukemia: clinical significance and progress to date. *Med Res Rev*. 2015;35(3):586-618.

SUPPORTING INFORMATION

Additional supporting information may be found online in the Supporting Information section at the end of the article.

How to cite this article: Romo-Morales A, Aladowicz E, Blagg J, Gatz SA, Shipley JM. Catalytic inhibition of KDM1A in Ewing sarcoma is insufficient as a therapeutic strategy. *Pediatr Blood Cancer*. 2019;e27888. <https://doi.org/10.1002/pbc.27888>